HHS Public Access

Author manuscript

Vaccine. Author manuscript; available in PMC 2016 October 05.

Published in final edited form as:

Vaccine. 2015 October 5; 33(41): 5386–5395. doi:10.1016/j.vaccine.2015.08.062.

Anti-Tumor Effect of the Alphavirus-based Virus-like Particle Vector Expressing Prostate-Specific Antigen in a HLA-DR Transgenic Mouse Model of Prostate Cancer

V. Riabov[1], **I. Tretyakova**[3], **R. B. Alexander**[1,2], **P. Pushko**[3], and **E. N. Klyushnenkova**[1,2]

[1]Department of Surgery, Division of Urology, University of Maryland School of Medicine

[2]VA Maryland Health Care System, Baltimore

[3]Medigen, Inc., Frederick, MD, USA

Abstract

The goal of this study was to determine if an alphavirus-based vaccine encoding human Prostate-Specific Antigen (PSA) could generate an effective anti-tumor immune response in a stringent mouse model of prostate cancer. *DR2bxPSA* F_1 male mice expressing human *PSA* and *HLA-DRB1*1501* transgenes were vaccinated with virus-like particle vector encoding PSA (VLPV-PSA) followed by the challenge with Transgenic Adenocarcinoma of Mouse Prostate cells engineered to express PSA (TRAMP-PSA). PSA-specific cellular and humoral immune responses were measured before and after tumor challenge. PSA and CD8 reactivity in the tumors was detected by immunohistochemistry. Tumor growth was compared in vaccinated and control groups. We found that VLPV-PSA could infect mouse dendritic cells *in vitro* and induce a robust PSA-specific immune response *in vivo*. A substantial proportion of splenic CD8+ T cells (19.6±7.4%) produced IFNγ in response to the immunodominant peptide $PSA_{65–73}$. In the blood of vaccinated mice, 18.4±4.1% of CD8+ T cells were PSA-specific as determined by the staining with H-$2D^b$/$PSA_{65–73}$ dextramers. VLPV-PSA vaccination also strongly stimulated production of IgG2a/b anti-PSA antibodies. Tumors in vaccinated mice showed low levels of PSA expression and significant CD8 T cell infiltration. Tumor growth in VLPV-PSA vaccinated mice was significantly delayed at early time points (p=0.002, Gehan-Breslow test). Our data suggest that TC-83-based VLPV-PSA vaccine can efficiently overcome immune tolerance to PSA, mediate rapid clearance of PSA-expressing tumor cells and delay tumor growth. The VLPV-PSA vaccine will undergo further testing for the immunotherapy of prostate cancer.

Corresponding author: Elena N. Klyushnenkova, University of Maryland, School of Medicine, Department of Surgery, 10 S. Pine Street, MSTF 400A, Baltimore, Maryland 21201. Phone: 410-706-0755; FAX: 410-706-0311; eklyushnenkova@smail.umaryland.edu.

Conflict of interest statement.

There are no conflicts of interest among the authors regarding the work.

The content is solely the responsibility of the authors and does not necessarily represent the official views of the funding agencies.

Keywords

TC-83 virus; VLPV; PSA; prostate cancer; vaccine; DR2b mice

Introduction

Prostate cancer is the second most frequently diagnosed cancer in men worldwide and sixth leading cancer-related cause of death in males [1]. Standard treatment options for prostate cancer patients when the disease is localized to the gland include radical prostatectomy, radiation and hormonal therapy [2]. Treatments for prostate cancer that has extended outside of the prostate are rarely curative, and the majority of patients eventually demonstrate progressive disease. The development of effective strategies for the control of prostate cancer is essential for public health, and alternative therapeutic approaches are urgently needed. Animal and clinical studies suggested that immunological approaches can be useful for prostate cancer treatment [3]. Current immunotherapeutic strategies include application of peptide-based, DNA-based and whole tumor cell vaccines targeting tumor-associated antigens, as well as dendritic cell-based therapies and immune check-point blockade [4;5]. Several immune-modulating agents (Sipuleucel-T, PROSTVAC-VF, GVAX, Ipilimumab) alone or in combinations with other therapeutic modalities showed efficacy against advanced prostate cancer in clinical trials [6].

The development of immunotherapy for prostate cancer based on the induction of autoimmunity to prostate-specific differentiation antigens is an attractive concept because prostate is not a vital organ beyond the reproductive years. PSA represents a promising target for the development of the prostate cancer-specific vaccine and immunotherapy because of its highly restricted expression on prostate tumor cells and normal prostate [7;8]. The development of prophylactic vaccination against prostate-specific differentiation antigens including PSA is a perspective strategy specifically for the treatment of prostate cancer. Men with detectable and rising PSA levels after radical prostatectomy as their only indication of recurrent prostate cancer have a high risk of progression to bone metastasis. Their median time to development of bone metastases is 8 years [9]. In that time these men are clinically well and immunologically intact, they would be ideal candidates for a preventive vaccine therapy that could delay progression without necessarily curing them. Previously, attempts to develop PSA-based vaccines for prostate cancer have been made using various viral vectors such as vaccinia/fowlpox virus or adenovirus [10;11] as well as other platforms [12;13]. Although promising anti-tumor and immune responses have been observed in these studies, the majority of approaches had limitations including strong antibody responses to the vectors [14;15].

Alphaviruses are single-stranded RNA viruses that belong to Togaviridae family. Their RNA genome contains non-structural genes responsible for transcription and replication of viral RNA, and structural genes encoding capsid and envelope proteins. Several members of alphavirus genus including Venezuelan equine encephalitis virus (VEEV) were used to develop experimental cancer vaccines [16]. Alphavirus replicons expressing tumor-specific antigens can be encapsulated into replicon particles, which essentially represent virus-like

particle vectors (VLPV) capable of delivering and expressing therapeutic antigens *in vitro* or *in vivo*. The construction of non-replicative alphavirus replicon vectors lacking expression of structural genes resulted in the minimization of pre-existing anti-vector immune responses and assured higher safety of alphavirus-based vaccines [17]. Moreover, inability of RNA-based expression vectors to integrate into host genome and induce insertional mutagenesis is another advantage of alphavirus-based platforms. Using this platform we have previously demonstrated that expression of several heterologous antigens (glycoproteins of Ebola and Lassa viruses, influenza virus hemagglutinin) by alphavirus-based vectors induced strong protective immunity against corresponding viral infections [17;18].

Previous studies demonstrated that effective protection and treatment of prostate cancer likely depended on the elicitation of effective CTL responses with the involvement of antigen-presenting dendritic cells (DC). The ability of vaccine-relevant antigens to enter DC was shown to be one of the critical requirements for a successful cancer immunotherapy [19;20]. Therefore, certain advantage of VEEV-based vectors is their preferential tropism towards lymphoid tissue [21;22]. This platform demonstrated efficiency in targeted gene delivery to DC and induction of protective immunity against several human viral pathogens [18;21]. Moreover, it was demonstrated that replicon-based vaccine overcame intrinsic tolerance to “self” tumor antigen Her2/neu and provided protection in a rat model of breast cancer [23]. Anti-tumor efficacy of the replicon particles encoding mutated human papilloma virus (HPV) 16 E6 and E7 genes has been also demonstrated in a HPV16 E6(+)E7(+) tumor challenge models [24]. Replicon particles encoding prostate Six-Transmembrane epithelial Antigen of the Prostate (STEAP), Prostate Stem Cell Antigen (PSCA) and Prostate Specific Membrane Antigen (PSMA) demonstrated strong immunogenicity and protective and therapeutic effects in a TRAMP mouse model [25;26]. Though PSA was previously shown to be relevant tumor antigen which induces CD8+ T cell response, and has very specific expression in the prostate [27], replicon-based PSA vaccines have never been extensively tested in preclinical models. In part, this was due to safety concerns associated with vectors derived from human pathogens. Unlike other studies, we used vectors derived from the TC83 vaccine, a live attenuated vaccine used under Investigational New Drug protocol for vaccinating personnel at risk of VEEV infection. In the present study, we demonstrate that the PSA-encoding VLPV derived from the TC-83 vaccine could efficiently overcome tolerance to the “self” antigen and induced strong PSA-specific CD8 T cell and Th1-type (IgG2a/b) antibody responses in a stringent transgenic mouse model with neonatal tolerance to PSA. In addition, preventive vaccination with the VLPV-PSA resulted in the elimination of PSA-expressing tumor cells and significantly delayed tumor growth in a stringent mouse model of prostate cancer in *DR2bxPSA* F_1 mice.

Materials and Methods

Preparation of the VLPV-PSA vaccine

VLPV-PSA vectors were prepared in CHO cells expressing TC-83 capsid and glycoproteins. TC-83 replicon vector was prepared by cloning human PSA gene downstream from the TC-83 subgenomic 26S promoter. Replicon RNA was made by using RNA transcription *in*

vitro and electroporated into CHO cells as described previously [17;28]. Briefly, 8 $\times 10^6$ cells were electroporated in 0.4 cm electrode gap cuvettes with three pulses of 0.85 kV at 25 uFD (Gene Pulser, BioRad). Transfected cells were incubated in 75 cm^2 flasks, and the culture supernatants were harvested at 30 h after transfection. To determine the VLPV titers, serial 10-fold dilutions were prepared and used to infect CHO cell monolayers in 8-chamber slides. After 24 hr incubation, cells were fixed with acetone followed by immunofluorescence assay (IFA) using antibodies to human kallikrein-3 (PSA) (R&D Systems, Minneapolis, MN). The titers were expressed as a number of infectious units (IU) per ml.

In vitro infection of dendritic cells and confocal microscopy

CD11c+ cells were enriched from the naïve mouse splenocytes by positive immunomagnetic selection. Adherent cells were treated with VLPV-PSA (5×10^5 IU/ml) or left untreated, and cultured in a chamber slide in a presence of 2×10^3 U/ml of mouse GM-CSF (BioLegend, San Diego, CA). Two hours post-infection, Brefeldin A (eBioscience, San Diego, CA) was added into chamber wells in the concentration 3 μg/ml. Cells were cultured for 24 h at 37°C, 5%CO_2. Slides were fixed with acetone. CD11c and PSA expression was detected by immunofluorescent staining using biotinylated hamster anti-mouse CD11c (clone N418, eBioscience) and goat anti-human PSA (R&D Systems) abs for 1 h, RT followed by addition of Streptavidin-Cy3 and donkey anti-goat Cy2 abs (both Jackson Immunoresearch Laboratories, West Grove, PA) for 45 min, RT. Nuclei were counterstained by NucBlue Live Cell Stain reagent (Molecular Probes, Eugene, OR). Images were acquired on the Zeiss LSM700 confocal microscope (40x water objective) using ZEN software.

Immunizations and tumor challenge experiments

All animal studies have been approved by the University of Maryland Institutional Animal Care and Use Committee. *DR2b×PSA* F_1 mice were generated by breeding *DR2b tg* and *PSA tg (B6)* mice as described previously [29]. *DR2bxPSA* F_1 male mice were randomly assigned to either vaccine or control groups, and immunized intramuscularly (i.m.) with 1×10^6 IU of VLPV-PSA unless indicated otherwise in the text. Secondary (boost) vaccination with 1×10^6 IU VLPV-PSA was performed four weeks later. Control groups received PBS at both time points. TRAMP tumor cell line engineered to express human PSA (TRAMP-PSA) was provided by Dr. J. Medin (University of Toronto, Canada) [30]. Tumor inoculation and monitoring was performed as described [29;31]. Mice were inoculated subcutaneously (s. c.) in the dorsal neck area with TRAMP-PSA cells (3×10^6 cells per mouse). Tumor growth was monitored by physical measurements weekly for up to 15 weeks. Tumor base area was calculated by measuring two bisecting diameters of the tumor and multiplying these values. Since TRAMP tumors have a tendency to ulcerate and bleed at relatively early time points, survival experiments were not performed due to animal welfare concerns and IACUC regulations. Instead, a tumor base area of 100 mm^2 was used as a surrogate end point for survival. For the immunohistochemical studies of tumors on early time-points, mice were inoculated with TRAMP-PSA tumor cells mixed with phenol-red free BD Matrigel Matrix (BD Bioscience, San Jose, California).

Immunological methods

IFN-γ ELISPOT assay, intracellular cytokine staining (ICS) and anti-PSA antibody ELISA were performed as described previously [29;31;32]. The anti-PSA Ab titers were calculated for individual plasma samples that gave a positive optical density ($OD_{405/650}$) ≥ 0.3 at 1/90 dilution. These samples were tested using serial 3-fold dilutions in the range from 1/90 to 1/21,870. The cutoff for these samples was calculated using the mean $OD_{405/650}$ of the negative samples plus 3 standard deviations. Two negative samples, each consisting of a pool of the plasma from 3 naïve mice, were tested, and values from all serial dilutions were used in calculation (12 values total). The dilution of the test sample corresponding to the cut-off OD was calculated from the titration curves by second order polynomial or power regression analysis using Excel software (R^2>0.95).

Dextramer staining

Heparinized peripheral blood was stained with H-2 D^b/HCIRNKSVI/PE PSA dextramer (Dxt/$PSA_{65–73}$, Immudex, Copenhagen, Denmark) followed by staining with anti-CD8-FITC (clone KT15, Santa Cruz Biotechnology, Dallas, Texas), anti-CD62L-Alexa Fluor 647 (BioLegend) and a mixture of PerCP-Cy5.5 labeled anti-CD11b, anti-CD19 (eBioscience), anti-CD4 (BD Bioscience) antibodies (“dump” channel). Red blood cells were lysed using 1X BD FACS Lysing Solution (BD Bioscience). Samples were analyzed using FACSCalibur flow cytometer (BD Bioscience) and CellQuest and FlowJo software.

Immunohistochemical (IHC) staining

Matrigel tumor implants were snap-frozen in isopentane on dry ice. To detect PSA, the cryosections were stained with the goat anti-human PSA Ab (R&D Systems) followed by the horseradish peroxidase (HRP)-labeled anti-goat Ig ImmPRESS reagent (Vector Laboratories, Burlingame, CA). To detect CD8, sections were stained with the rat anti-mouse CD8 mAb (clone 53-6.7, BD Biosciences) followed by the HRP-labeled goat anti-rat IgG antibodies (Santa Cruz Biotechnology). Sections were developed using the AEC staining kit (Sigma-Aldrich, St. Louis, MO) and counterstained by the Mayer’s Haemalaun solution (AppliChem, St. Louis, MO). Images were taken using the Zeiss Axioskop microscope and AxioVision 3.0 software. For the quantification of PSA and CD8 staining, series of images spanning the entire Matrigel section were taken at 2.5x magnification and scanned using the Aperio ImageScope software and Positive Pixel Count Algorithm (Hue value = 0.1, color saturation threshold = 0.1). The intensity of staining (positivity) per image was expressed as number of positive pixels divided by total number of pixels. Average intensity per section was calculated for each mouse using 2–6 images (depending on the section size).

Statistical analysis

For the ELISPOT assay, means and SD of triplicates were calculated for individual mice. The specific responses from these mice were compared to background responses in the absence of antigen using a two-sided Student *t-test* at P<0.05 level. Frequencies of the IFN-γ producing cells per 1×10^6 cells were calculated by the equation: [(spot $number_{sample}$ - average spot number, $_{No\ antigen}$)/number of replicates]×[1×10^6/number of cells per well].

Survival, using a tumor base of 100 mm^2 as a surrogate marker, was calculated by polynomic regression analysis using Excel software (R-squared values > 0.95). Time-to-event analysis was performed on imputed time values by Gehan-Breslow and log rank tests using SigmaPlot 12.0 software (Systat Software, Inc., San Jose, CA). The ANOVA analyses and the test for the homogeneity of variance were performed using SAS 9.3 software (SAS Institute, Cary, NC).

Results

Preparation of virus-like particle vectors expressing PSA (VLPV-PSA) and in vitro infections

The VLPV-PSA particles that contained TC-83 replicons encoding PSA gene were generated in CHO cells that expressed the structural proteins (capsid and glycoproteins) of TC-83 alphavirus. Under these conditions, the TC-83 structural proteins formed virus-like particles and encapsulated the TC-83 replicons encoding PSA gene into VLPV-PSA vectors. The schema of the vector is shown in Figure 1A. Based on the full-length human PSA protein (GeneBank AAG33355) (wtPSA), a synthetic gene was designed to express the codon-optimized PSA (coPSA) with the amino acid sequence identical to the wtPSA. The RNAs for the PSA expression vector and gp- and c-helpers were prepared by *in vitro* transcription. The TC-83 vector expressing wtPSA was used as a control. The quality of RNAs was confirmed on 1% agarose gel (Figure 1B). In order to characterize the kinetics of PSA secretion, CHO cells were transfected with replicon vector RNA, and supernatants from the RNA-transfected cells were collected at different time points for the analysis by SDS-PAGE and Western blot. The results are shown in Figure 1D. Both wtPSA and coPSA were detected in the conditioned medium. A coPSA was expressed at approximately 10-fold higher level compared to the wild type PSA.

The ability of VLPV to deliver PSA genes to the cells and to express PSA was first determined by transducing CHO cells with VLPV-PSA *in vitro*. The VLPV-PSA vectors were harvested from the CHO cell growth medium, concentrated, and quantitated in CHO cell monolayers by indirect immunofluorescent staining (IFA). Expression of PSA was detected in individual CHO cells; no spreading of expression to adjacent cells was detected (Supplemental Figure 1A). The titers of VLPV-PSA particles were approximately $1–5\times10^8$ infectious units (IU)/ml.

Since the VLPV vector system was derived from the TC-83 vaccine strain of VEE virus, which has been shown to target lymph nodes *in vivo* including DC [33–35], we tested VLPV-PSA for the ability to deliver and express PSA genes in human monocytic myeloid cells (MMCs) and mouse DCs (Supplemental Figure 1B, C). Human MMCs were differentiated from CD14-enriched peripheral blood mononuclear cells using rhGM-CSF and rhIL4. Non-adherent cell fraction enriched in DCs was used for the *in vitro* infection. As shown in Supplemental Figure 1B, numerous positive cells were detected suggesting that VLPV-PSA can deliver and express PSA gene in human MMCs. To further confirm that VLPV-PSA may target antigen-presenting cells, we isolated CD11c+ DCs from mouse spleens and used them in the *in vitro* infection assay. Incubation of primary mouse splenic DCs with VLPV-PSA for 24 h resulted in the robust accumulation of PSA in the cytoplasm

of CD11c+ cells as detected by IFA and confocal microscopy. In contrast, CD11c+ cells incubated without VLPV-PSA did not show PSA reactivity (Supplemental Figure 1C). These data indicated that VLPV-PSA are able to infect mouse DCs and induce production of heterologous antigen (PSA).

Immunogenicity of VLPV-PSA vaccine in vivo in DR2bxPSA F_1 mice

In order to test the effects of immunization with VLPV-PSA vaccine on the development of anti-PSA immune responses we utilized *DR2bxPSA F_1* double transgenic mice which express PSA as a "self" antigen, specifically in the prostate. Previously we have shown that these mice confer neonatal tolerance to PSA and are able to present PSA peptides both in the context of DR2b chimeric transgene and mouse endogenous H2-D^b molecules. *DR2bxPSA F_1* mice demonstrated a striking reduction in PSA-specific CD8 T cell responses and enhanced TRAMP-PSA prostate tumor growth compared to the wild type B6 mice. The expression of DR2b was associated with active suppression of the CTL response to the tumor antigen similar to that seen in human tumors. This represents a very stringent model for testing immunotherapy of prostate cancer [29;31].

In the preliminary studies, we tested *in vivo* effects of VLPV-PSA vaccine in a wide range of concentrations from 4×10^7 IU to 5×10^3 IU per dose. PSA-specific immune responses in the spleens and inguinal lymph nodes (LN) were measured two weeks after the second immunization. IFNγ production was first detected using the ELISPOT assay (Figure 2 and data not shown). The frequencies of IFNγ-producing cells in response to H-$2D^b$-restricted immunodominant PSA peptide ($PSA_{65–73}$) and irradiated TRAMP-PSA cells (irTRAMP-PSA) were significantly increased in the spleens of vaccinated mice compared to the controls (irrelevant peptide or parental TRAMP-C1 tumor cells respectively) (Figure 2A). Naive mice did not show detectable PSA-specific CD8 T cell response. Immunization with VLPV-PSA at 1×10^6–4×10^7 IU induced strong PSA-specific IFNγ production in the spleens; the responses gradually declined but were detectable at the lower dose range (4×10^4–4×10^5 IU/dose) (Figure 2A). In contrast to the overwhelmingly strong responses in the spleens, the levels of the response in the inguinal LN were much lower in magnitude, although the overall pattern of the dose response in the LN was similar to the one detected in the spleen (Figure 2B). While CD8 T cell and antibody responses to PSA were detectable in mice immunized with VLPV-PSA at the doses as low as 5×10^4 IU per mouse, we were not able to detect an IFN-γ effector CD4 T cell response to PSA at any doses tested (data not shown).

High doses of the vaccine ($\geq10^7$ IU) induced exhaustion of the mouse immune system, which manifested in the depletion of the lymph nodes and signs of vascular inflammation. However, the vaccination did not result in any apparent systemic toxicity based on the animal appearance and behavior during next 2 days following vaccination. None of the mice lost weight during a course of observation (data not shown). Lower vaccine doses (5×10^5–5×10^6 IU) did not cause any apparent adverse effects but potently induced PSA-specific IFNγ production in the ELISPOT assay.

PSA-specific CD8+ T cells were also detected directly in the peripheral circulation using H-$2D^b$ dextramers loaded with $PSA_{65–73}$ peptide. As shown in Figure 3A, a large proportion

(18.4±4.1%) of CD8 T cells in the blood of vaccinated mice was H-2D^b/PSA$_{65–73}$ dextramer positive, while naïve mice showed no specific reactivity. The majority (>98%) of H-2D^b/PSA$_{65–73}$ dextramer positive were CD62Llow T cells (presumably effector T cells). Strong PSA-specific CD8 T cell reactivity was also confirmed by the ICS. In vaccinated mice, a significant proportion of splenic CD8 T cells (19.6±7.4%) produced IFNγ in response to the specific peptide PSA$_{65–73}$, while the responses were at the background level in control mice (Figure 3B). The responses to the polyclonal stimulation with PMA/Ionomycin were strong in both vaccinated and control groups (data not shown).

To test humoral immune responses after VLPV-PSA vaccination, PSA-specific antibody titers in the serum were analyzed by ELISA (Figure 3C). Vaccinated mice had high titers of PSA-specific antibodies with predominance of IgG2a sub-isotype. IgG1 Abs were detected in 58% (7 out of 12) samples, with the geometric mean titer for positive samples 1,024. All tested mice developed strong IgG2a Ab response to PSA (mean titer 20,201, n=12), and 92% mice (11 out of 12) developed IgG2b Ab response (mean titer for positive samples 8,732). Naïve mice showed no detectable PSA-specific antibody responses (data not shown).

The comparison of two vaccine doses (6×10^6 IU and 1×10^6 IU) did not reveal significant differences in the magnitude of PSA-specific CD8 T cell response as determined by the percentages of IFNγ-producing CD8+ T cells in the spleen by the ELISPOT assay and by ICS or by comparison of the titers of anti-PSA antibodies in the plasma (data not shown). Therefore, two i.m. injections of VLPV-PSA at 1×10^6 IU per dose delivered 4 weeks apart was used in all subsequent tumor challenge experiments.

VLPV-PSA vaccination results in the efficient elimination of PSA-expressing tumor cells and delayed tumor growth in vivo in DR2bxPSA F_1 mice

Since VLPV-PSA vaccination induced strong PSA-specific cellular and humoral immune responses, we next tested if this could result in elimination of implanted TRAMP tumor cells expressing PSA. TRAMP-PSA cells injected subcutaneously do not produce palpable tumors for several weeks after inoculation. However, we assumed that efficient anti-tumor response, if present, should develop at early time-points after tumor challenge. In order to trace immunological events in the tumor at early time-points, *DR2bxPSA F_1* male mice were injected with TRAMP-PSA tumor cells impregnated in Matrigel. This technique allows the characterization of the infiltrating immune cells in the tumor. Matrigel plugs were harvested at different time points after tumor inoculation. As early as 7 days after tumor challenge, IHC staining for PSA revealed strong reactivity in the control (PBS) samples, which was especially intensive on the margins of Matrigels. In contrast, tumor-impregnated Matrigel plugs from vaccinated mice exhibited little PSA reactivity (Supplemental Figure 2). The most striking differences in the Matrigel plug structure between control and vaccinated mice were detected 3 weeks after TRAMP-PSA injection. Samples from control mice contained dense areas of tumor growth with high overall cellularity and bright PSA reactivity. In contrast, Matrigels from vaccinated mice demonstrated greatly reduced overall cellularity and strong decrease in PSA reactivity indicating efficient clearance of PSA-expressing tumor cells (Supplemental Figure 2). The images that span the entire tissue sections at 2.5x magnification were taken for each animal, and the intensity of staining was quantified using

Aperio ImageScope software and Positive Pixel Count Algorithm (Figure 4A). The intensity of positive staining among all 6 groups (vaccine versus control treatment at 3 time points) was compared by the ANOVA. For the PSA staining, the results of the overall ANOVA test indicated that the difference between groups was statistically significant ($F_{3,14}$=7.92, p=0.0025). The global effect of the vaccination was highly statistically significant (least square means for the PSA staining intensity 0.001 and 0.009 for the control and vaccine groups respectively, $F_{1,14}$=18.41, p=0.0007*).* However, pairwise comparisons between vaccinated and non-vaccinated groups at each time point were only marginally significant (0.05<p<0.1, Satterthwaite t-test). Within the treatment groups, the effect of time was also non-significant (ANOVA F test).

Similar analysis was performed for the Matrigel tumor sections from the same mice stained with anti-CD8 mAb (Figure 4B). In mice that received VLPV-PSA vaccine, lack of the PSA reactivity on day 7 post-tumor inoculation was associated with substantial CD8+ cells infiltration, while CD8+ cells infiltration in control samples was undetectable at this time-point (Supplemental Figure 3). The same tendency in PSA expression and CD8+ cell infiltration was observed 2 weeks after tumor cell inoculation. CD8+ cell infiltration of Matrigels from control mice was delayed and became visually detectable only 23 days after injection. Interestingly, at this time-point CD8+ cell infiltration of Matrigel plugs in vaccinated animals decreased suggesting that the peak of the effector phase of the anti-tumor response occurred early after tumor challenge (Supplemental Figure 3). However, the quantitative analysis of the CD8 staining intensity indicated that the difference between groups for the CD8 positivity was not statistically significant ($F_{3,13}$=1.2, p=0.347) (Figure 4B).

In order to characterize tumor growth in control and vaccinated groups, we have performed time-to-event (“survival”) analysis using a tumor base of 100 mm^2 as a surrogate endpoint. Four independent experiments were performed, each showing an identical trend of delayed tumor growth in vaccinated mice during early time points (weeks 2–7). Median time-to-event (tumor base of 100 mm^2) for individual experiments is shown in Table 1. Since all four experiments were performed under similar conditions, and there was no violation of the assumption of homogeneity of variance (p =0.15), we combined the data from all experiments for the time-to-event analysis (Figure 5). Vaccination with VLPV-PSA resulted in a statistically significant delay of TRAMP-PSA tumor growth at early time points (Gehan-Breslow test, p = 0.002). However, the differences in the median time-to-event were modest. Median time-to-event for the control group was 7.2 weeks (95% confidence interval (CI) 6.5, 7.9). Median time-to-event for the vaccine group was 8.6 weeks (95% CI 7.6, 9.5), and the log rank test showed only marginally significant difference between the survival curves (p=0.059).

In order to study the mechanism of tumor outgrowth in vaccinated mice on the late stages after tumor challenge we examined whether injection of VLPV-PSA favors immune selection of PSA-negative tumor variants. Solid TRAMP-PSA tumors were harvested nine or ten weeks after tumor challenge and subjected to IHC analysis for the PSA expression. Tumors from both VLPV-PSA vaccinated and control mice contained areas of bright PSA reactivity suggesting outgrowth of PSA-expressing tumor cells (Supplemental Figure 4).

These results suggested that relapse of tumor growth in vaccinated mice was not caused by immune selection of PSA-negative tumor cells but rather indicate the lack of robust PSA-specific effector immunity inside tumor tissue.

We also determined the frequency of PSA-specific CD8 T cells the in the peripheral blood at different time points after tumor inoculation by staining with H-2D^b/PSA$_{65–73}$ Dxt. As shown in Figure 6A, vaccination with VLPV-PSA resulted in the very high level of circulating PSA-specific CD8 T cells at all-time points measured. The highest frequency of PSA-specific CD8 T cells in the peripheral blood was observed at week 2 after tumor inoculation ($p=0.04$ compared to week 1, ANOVA). The vast majority (99%) of PSA$_{65–73}$-specific CD8+ cells in vaccinated mice retained CD62L^{low} phenotype (data not shown). The frequencies of IFNγ-producing CD8 T cells in the spleens upon PSA$_{65–73}$ peptide stimulation were also very high in vaccinated mice compared to the controls as measured by the ELISPOT assay and ICS (Figure 6B and C respectively). The majority of IFNγ-producing CD8 T cells in the spleen also produced TNFα (12.3±5.7%) indicating that the vaccine induced polyfunctional effector cytokine response (Figure 6C). IFNγ-producing CD8 T cells were also clearly detectable in the tumor-draining lymph nodes (cervical/axillary), however the magnitude of the responses was about 10-fold lower compared to the spleen (Figure 6B). These data suggested that the vaccination with VLPV-PSA induced a very potent systemic CD8 T cell response.

Discussion

In the current study we used a recently developed mouse model with established neonatal tolerance to human PSA (*DR2bxPSA F_1*) [29] to evaluate a novel alphavirus-based PSA-encoding vaccine against prostate cancer. We demonstrated that despite diminished immunogenicity of PSA expressed as a “self” antigen in our model, VLPV-PSA vaccine induced a potent PSA-specific anti-tumor response that resulted in the significant delay of TRAMP-PSA tumor growth specifically at early stages. We also showed that immunization with TC-83-based VLPV encoding a full-length human PSA induced strong CD8 T cell and Th1-type polarized IgG2a/b antibody responses in *DR2bxPSA F_1* mice. *In vitro* studies demonstrated that VLPV-PSA vaccine was able to target and express heterologous antigen (PSA) in primary CD11c+ DC. To the best of our knowledge, this report is the first study describing expression of PSA from VEE replicon vector and its immunogenicity in a mouse model with neonatal tolerance to PSA.

The ability to induce very strong antigen-specific cellular responses can be distinctive characteristic of alphavirus-based vaccines. Our data are in concordance with previously reported preclinical and clinical studies that demonstrated efficacy of alphavirus-based vaccines in breaking immunological tolerance, induction of potent immune responses against tumor antigens, and inhibition of tumor growth [23;36;37; 38]. For instance, in line with our results, PSMA-expressing vaccine against prostate cancer induced robust CD8+ T cells responses in a preclinical study [38].

In that study, a virus replicon particle (VRP) vaccine based on attenuated VEEV encoding human PSMA has been shown to induce Th-1 cytokines, strong CTL response, and IgG2a/

IgG2b antibodies at relatively low VRP doses in BALB/c and C57BL/6 mice [38]. In contrast, a study by Garcia-Hernandez *et al.* showed that combination of the vaccination with mouse STEAP encoded by the naked DNA vector followed by the boost with the VEEV-based STEAP-VRP induced only modest CD8 T cells response, which also required *in vitro* IL-2 stimulation [39]. CD4 T cells but not CD8 T cells appeared to be critical for the anti-tumor effect of the vaccine in this model, although the induction of a STEAP-specific CD4 T cell response was not directly demonstrated in this study [39]. In a similar study by the same group, vaccination with the mouse PSCA-encoding naked DNA/VRP combination induced stronger PSCA-specific CD8 T cell responses [40]. Potent anti-tumor effects accompanied by strong cellular and humoral responses have recently been demonstrated in mouse model of B16 melanoma after vaccination with VEEV-based vaccine targeting “self” tumor antigen TRP2 [41].

In our experiments, the magnitude of the IFNγ CD8 T cell response to PSA in the spleens induced by two immunizations with the TC-83-based VLPV-PSA was several times higher compared to the frequencies reported in other studies (approximately 1,500 spots per 1×10^6 of unfractionated splenocytes in the ELISPOT assay), and was detected in a direct 48-hr assay without a prolonged *in vitro* stimulation. In our study, strong PSA-specific CD8 T cell responses were detected in the spleens as early as 1 week and peaked at 2 weeks post-treatment. At this time, approximately 20% of CD8+ gated population in the peripheral blood of vaccinated mice stained positively for H2-D^b dextramers loaded with $PSA_{65–73}$ peptide and exhibited $CD62L^{low}$ phenotype, the characteristic of antigen-specific effector T cells. Moreover, vigorous CD8+ T cell responses to PSA did not decrease after tumor challenge. A high frequency of PSA-specific CD8+ T cells in the blood was observed in vaccinated mice during at least the first 3 weeks after tumor cell inoculation. Splenic CD8+ T cells from these mice were characterized by the potent polyfunctional (IFNγ/TNFα) PSA-specific responses. In contrast, Durso *et al*. reported that the VRP-induced PSMA-specific CTL responses were detected after 5 days of *in vitro* expansion [38]. In that study, 3 immunizations were required for the induction of strong responses, although the dose of VRP-PSMA was much lower (2×10^5 IU). It is not clear whether discrepancies between our studies were related to the vector construction, the method of determining the VLPV titer, or the differences in the antigen epitope composition.

Strong IgG2a/b antibody responses were also detected in all mice vaccinated with VLPV-PSA in our model. We have observed a remarkable heterogeneity in the IgG1 response, while IgG2a responses were relatively homogeneous and very high. We suggest that this reflects a process of isotype switching from IgG1 to IgG2a to IgG2b sub-isotypes induced by the vaccine, the kinetics of which may vary in individual mice. However, we were unable to detect measurable IFN-γ CD4 T cell responses using whole PSA or immunodominant DR2b-restricted peptides $PSA_{171–190}$ and $PSA_{221–240}$. Yet, the presence of the strong IgG2a/b antibody response suggested that helper CD4 T cells were activated by the VLPV-PSA vaccine.

The applicability of PSA as a target antigen for prostate cancer therapy was previously demonstrated in mouse models of prostate cancer using several PSA-expressing vector platforms [42]. Elzey *et al.* showed that adenoviral (Ad)5-PSA-based vaccine induced anti-

tumor effect in the RM11 tumor model when delivered in combination with cytokine (IL-2, IL-12, TNFα) therapy. In this study, potent CTL responses to PSA were induced only by high vector doses (1×10^7–1×10^9 plaque-forming units) and required *in vitro* CTL expansion [42]. The induction of the PSA-specific anti-tumor immune response by the PSA-expressing polyomavirus virus-like particles in D2F2 tumor model has been recently reported by Eriksson *et al*. [43]. However, the reported responses were low. In that study, IFNγ PSA-specific CD4 T cell reactivity was also demonstrated. Importantly, in these and some other models, PSA appeared to be a foreign antigen, which could predispose immune system to the induction of the strong immune responses in the absence of neonatal tolerance [13;38;42–44]. Previously, we have tested PSA vaccine based on live mouse CMV vector in *DR2bxPSA* F_1 mouse model [29]. Compared to the CMV vector, the TC83-based vaccine induced much more robust CD8+ T cell response to PSA despite the fact that TC83-based particles cannot propagate inside the cells.

In the current study we used a stringent and clinically relevant mouse model of prostate cancer with established neonatal tolerance to PSA. We believe this model to be highly suitable for testing anti-tumor effects of PSA-encoding vaccine for several reasons. First, we have previously demonstrated that human HLA-DRB1*1501 (DR2b) is a permissive allele for PSA, whereas mouse endogenous I-A^b allele could not accommodate a strong CD4 T cell response to PSA [31]. As a consequence, single PSA transgenic mice of B6 origin rejected TRAMP-PSA tumors whereas simple presence of DR2b transgene in *DR2bxPSA* F_1 double transgenic mice resulted in a progressive growth of TRAMP-PSA tumors [29;31]. We hypothesized that this was due to a combination of the diminished CD8 T cell reactivity to “self” antigen expressed in the prostate and the DR2b-mediated immunosuppression. In fact, we have recently demonstrated that depletion of CD4+CD25+ regulatory T cells significantly delayed TRAMP-PSA tumor growth, especially when used in combination with CTL-associated antigen (CTLA)-4 blockade [45]. On the other hand, myeloid suppressor cells were unlikely to be involved in the inhibition of anti-tumor immunity at early time points, since tumor-associated macrophages displayed immuno-stimulatory anti-tumor phenotype during early tumor progression in our model [46]. Our results demonstrated that despite of the induction of neonatal tolerance to PSA and active immunosuppression in *DR2bXPSA* F_1 mice, vaccination with a relatively low dose of TC-83 based VLPV-PSA (1×10^6 IU) induced strong PSA-specific CD8+ T cell-mediated immune responses in the spleen and peripheral blood of vaccinated animals.

Despite strong PSA-specific cellular and humoral responses induced by VLPV-PSA vaccine, its effect on tumor growth was moderate. This result may reflect stringency of our experimental model and effects of PSA expressed as a “self” antigen. Thus, additional administration of the vaccine may be required in order to facilitate anti-tumor effect. Furthermore, although tumor cell line used in our study showed high efficiency of PSA expression (>90% of positive cells), and tumors dissected at the end of the observation period were PSA-positive, we cannot completely exclude a possibility of immuno-editing and escape of PSA-negative or low PSA-expressing poorly immunogenic tumors. Lastly, despite high frequency of antigen-specific CD8+ T cells in the spleens and peripheral blood of vaccinated mice, the PSA-specific reactivity was relatively low in the tumor draining

lymph nodes. Tumor implants from VLPV-PSA vaccinated mice contained more CD8+ cells than control mice at week 1 after tumor cell inoculation. However, intensity of CD8+ cell infiltration in vaccinated animals was modest and visually decreased at weeks 2 and 3. These data suggest that influx of PSA-specific CD8 T cells into the tumor also may be insufficient. Optimization of VLPV-PSA construct and combinatory approaches which include treatment with vaccine and other immunostimulatory drugs may also enhance anti-tumor effect of VLPV-PSA vaccine.

In our study, high doses of the VLPV-PSA vaccine induced signs of inflammation detected by post-mortem examination. The VEE-based VLP encoding PSMA has been tested in a phase I clinical trial in patients with CRPC metastatic to bone. No toxicities were observed during the treatment which included five doses of the VLPV-PSMA (0.9×10^7 IU or 0.36×10^8 IU). However, lack of clinical benefits and low immune signals in that study suggested that dosing was suboptimal [26]. The high VLPV doses that caused immune system exhaustion in mice should be included as one parameter for consideration to determine a human dose in the future clinical trial.

In summary, our results demonstrate that a novel alphavirus-based vaccine could efficiently break an immune tolerance to PSA and potentiate a rapid clearance of emerging PSA-expressing tumor cells on early stages after tumor challenge presumably due to efficiency of alphavirus vectors in the induction of CD8 T cell effector responses.

This observation indicates that PSA-specific immune surveillance in vaccinated animals is indeed increased and effector cells are able to eliminate PSA-expressing tumor cells. There are several clinical scenarios in patients with prostate cancer where this could be of particular relevance. For example, men with detectable and rising PSA after radical prostatectomy as their only indication of recurrent prostate cancer have a high risk of progression to bone metastasis. Their median time to development of bone metastases is 8 years [9]. In that time these men are clinically well and immunologically intact, they would be ideal candidates for a vaccine therapy that could delay progression without necessarily curing them. The VLPV-PSA vaccine tested in the current study is based on the attenuated vaccine (TC-83 strain) and can be directly tested in human subjects without further modifications. Recently, a prostate cancer vaccine based on attenuated VEEV strain was used in a phase I trial involving patients with metastatic CRPC and demonstrated good safety and tolerability [26]. We believe that our novel alphavirus-based VLPV-PSA vaccine warrants further testing for the treatment of prostate cancer.

Supplementary Material

Refer to Web version on PubMed Central for supplementary material.

Acknowledgments

Grant support: This study was supported in part by the NIH NCI contract HHSN261201100088C, a grant from the U.S. Department of Veterans Affairs, and the University of Maryland Marlene and Stewart Greenebaum Cancer Center's Paul Calabresi Fellowship in Clinical Oncology.

The authors thank Dr. Rachmat Hidajat, Dr. Rikka Saito, and Brian Nickols for their valuable contributions and technical support.

Abbreviations

PSA	Prostate-Specific Antigen
VLPV-PSA	virus-like particle vector encoding PSA
TRAMP-PSA	Transgenic Adenocarcinoma of Mouse Prostate cells engineered to express PSA
VEEV	Venezuelan equine encephalitis virus
STEAP	Six-Transmembrane epithelial Antigen of the Prostate
PSCA	Prostate Stem Cell Antigen
PSMA	Prostate Specific Membrane Antigen
ICS	intracellular cytokine staining
Dxt	dextramer

Reference List

1. Jemal A, Bray F, Center MM, Ferlay J, Ward E, Forman D. Global cancer statistics. CA Cancer J Clin. 2011 Mar; 61(2):69–90. [PubMed: 21296855]
2. Wilt TJ, Ahmed HU. Prostate cancer screening and the management of clinically localized disease. BMJ. 2013; 346:f325. [PubMed: 23360718]
3. Karan D, Holzbeierlein JM, Van VP, Thrasher JB. Cancer immunotherapy: a paradigm shift for prostate cancer treatment. Nat Rev Urol. 2012 Jul; 9(7):376–85. [PubMed: 22641164]
4. Gulley JL, Drake CG. Immunotherapy for prostate cancer: recent advances, lessons learned, and areas for further research. Clin Cancer Res. 2011 Jun 15; 17(12):3884–91. [PubMed: 21680544]
5. Cha E, Fong L. Immunotherapy for prostate cancer: biology and therapeutic approaches. J Clin Oncol. 2011 Sep 20; 29(27):3677–85. [PubMed: 21825260]
6. Madan RA, Heery CR, Gulley JL. Poxviral-based vaccine elicits immunologic responses in prostate cancer patients. Oncoimmunology. 2014; 3:e28611. [PubMed: 25097802]
7. Cunha AC, Weigle B, Kiessling A, Bachmann M, Rieber EP. Tissue-specificity of prostate specific antigens: comparative analysis of transcript levels in prostate and non-prostatic tissues. Cancer Lett. 2006 May 18; 236(2):229–38. [PubMed: 16046056]
8. Lilja H, Ulmert D, Vickers AJ. Prostate-specific antigen and prostate cancer: prediction, detection and monitoring. Nat Rev Cancer. 2008 Apr; 8(4):268–78. [PubMed: 18337732]
9. Pound CR, Partin AW, Eisenberger MA, Chan DW, Pearson JD, Walsh PC. Natural history of progression after PSA elevation following radical prostatectomy. JAMA. 1999 May 5; 281(17): 1591–7. [PubMed: 10235151]
10. Uhlman MA, Bing MT, Lubaroff DM. Prostate cancer vaccines in combination with additional treatment modalities. Immunol Res. 2014 Aug; 59(1–3):236–42. [PubMed: 24838261]
11. Kantoff PW, Schuetz TJ, Blumenstein BA, et al. Overall survival analysis of a phase II randomized controlled trial of a Poxviral-based PSA-targeted immunotherapy in metastatic castration-resistant prostate cancer. J Clin Oncol. 2010 Mar 1; 28(7):1099–105. [PubMed: 20100959]
12. Pavlenko M, Roos AK, Lundqvist A, et al. A phase I trial of DNA vaccination with a plasmid expressing prostate-specific antigen in patients with hormone-refractory prostate cancer. Br J Cancer. 2004 Aug 16; 91(4):688–94. [PubMed: 15280930]

13. Shahabi V, Reyes-Reyes M, Wallecha A, Rivera S, Paterson Y, Maciag P. Development of a Listeria monocytogenes based vaccine against prostate cancer. Cancer Immunol Immunother. 2008 Sep; 57(9):1301–13. [PubMed: 18273616]
14. Anderson RJ, Schneider J. Plasmid DNA and viral vector-based vaccines for the treatment of cancer. Vaccine. 2007 Sep 27; 25(Suppl 2):B24–B34. [PubMed: 17698262]
15. Nishimoto KP, Laust AK, Nelson EL. A human dendritic cell subset receptive to the Venezuelan equine encephalitis virus-derived replicon particle constitutively expresses IL-32. J Immunol. 2008 Sep 15; 181(6):4010–8. [PubMed: 18768856]
16. Quetglas JI, Ruiz-Guillen M, Aranda A, Casales E, Bezunartea J, Smerdou C. Alphavirus vectors for cancer therapy. Virus Res. 2010 Nov; 153(2):179–96. [PubMed: 20692305]
17. Pushko P, Parker M, Ludwig GV, Davis NL, Johnston RE, Smith JF. Replicon-helper systems from attenuated Venezuelan equine encephalitis virus: expression of heterologous genes in vitro and immunization against heterologous pathogens in vivo. Virology. 1997 Dec 22; 239(2):389–401. [PubMed: 9434729]
18. Pushko P, Geisbert J, Parker M, Jahrling P, Smith J. Individual and bivalent vaccines based on alphavirus replicons protect guinea pigs against infection with Lassa and Ebola viruses. J Virol. 2001 Dec; 75(23):11677–85. [PubMed: 11689649]
19. Heiser A, Coleman D, Dannull J, et al. Autologous dendritic cells transfected with prostate-specific antigen RNA stimulate CTL responses against metastatic prostate tumors. J Clin Invest. 2002 Feb 1; 109(3):409–17. [PubMed: 11828001]
20. Willis RA, Bowers WJ, Turner MJ, et al. Dendritic cells transduced with HSV-1 amplicons expressing prostate-specific antigen generate antitumor immunity in mice. Hum Gene Ther. 2001 Oct 10; 12(15):1867–79. [PubMed: 11589829]
21. Davis NL, Brown KW, Johnston RE. A viral vaccine vector that expresses foreign genes in lymph nodes and protects against mucosal challenge. J Virol. 1996 Jun; 70(6):3781–7. [PubMed: 8648713]
22. Caley IJ, Betts MR, Irlbeck DM, et al. Humoral, mucosal, and cellular immunity in response to a human immunodeficiency virus type 1 immunogen expressed by a Venezuelan equine encephalitis virus vaccine vector. J Virol. 1997 Apr; 71(4):3031–8. [PubMed: 9060663]
23. Nelson EL, Prieto D, Alexander TG, et al. Venezuelan equine encephalitis replicon immunization overcomes intrinsic tolerance and elicits effective anti-tumor immunity to the ‘self’ tumor-associated antigen, neu in a rat mammary tumor model. Breast Cancer Res Treat. 2003 Dec; 82(3): 169–83. [PubMed: 14703064]
24. Cassetti MC, McElhiney SP, Shahabi V, et al. Antitumor efficacy of Venezuelan equine encephalitis virus replicon particles encoding mutated HPV16 E6 and E7 genes. Vaccine. 2004 Jan 2; 22(3–4):520–7. [PubMed: 14670335]
25. Gray A, van de la Luz Garcia-Hernandez WM, Kanodia S, Hubby B, Kast WM. Prostate cancer immunotherapy yields superior long-term survival in TRAMP mice when administered at an early stage of carcinogenesis prior to the establishment of tumor-associated immunosuppression at later stages. Vaccine. 2009 Dec 30; 27(Suppl 6):G52–G59. [PubMed: 20006141]
26. Slovin SF, Kehoe M, Durso R, et al. A phase I dose escalation trial of vaccine replicon particles (VRP) expressing prostate-specific membrane antigen (PSMA) in subjects with prostate cancer. Vaccine. 2013 Jan 30; 31(6):943–9. [PubMed: 23246260]
27. Gulley JL, Madan RA, Tsang KY, et al. Immune impact induced by PROSTVAC (PSA-TRICOM), a therapeutic vaccine for prostate cancer. Cancer Immunol Res. 2014 Feb; 2(2):133–41. [PubMed: 24778277]
28. Kamrud KI, Alterson KD, Andrews C, et al. Analysis of Venezuelan equine encephalitis replicon particles packaged in different coats. PLoS One. 2008; 3(7):e2709. [PubMed: 18628938]
29. Klyushnenkova EN, Kouiavskaia DV, Parkins CJ, et al. A cytomegalovirus-based vaccine expressing a single tumor-specific CD8+ T-cell epitope delays tumor growth in a murine model of prostate cancer. J Immunother. 2012 Jun; 35(5):390–9. [PubMed: 22576344]
30. Medin JA, Liang SB, Hou JW, Kelley LS, Peace DJ, Fowler DH. Efficient transfer of PSA and PSMA cDNAs into DCs generates antibody and T cell antitumor responses in vivo. Cancer Gene Ther. 2005 Jun; 12(6):540–51. [PubMed: 15678150]

31. Klyushnenkova EN, Kouiavskaia DV, Berard CA, Alexander RB. Cutting edge: Permissive MHC class II allele changes the pattern of antitumor immune response resulting in failure of tumor rejection. J Immunol. 2009 Feb 1; 182(3):1242–6. [PubMed: 19155468]
32. Klyushnenkova EN, Link J, Oberle WT, et al. Identification of HLA-DRB1*1501-restricted T-cell epitopes from prostate-specific antigen. Clin Cancer Res. 2005 Apr 15; 11(8):2853–61. [PubMed: 15837732]
33. Grieder FB, Nguyen HT. Virulent and attenuated mutant Venezuelan equine encephalitis virus show marked differences in replication in infection in murine macrophages. Microb Pathog. 1996 Aug; 21(2):85–95. [PubMed: 8844652]
34. MacDonald GH, Johnston RE. Role of dendritic cell targeting in Venezuelan equine encephalitis virus pathogenesis. J Virol. 2000 Jan; 74(2):914–22. [PubMed: 10623754]
35. Nishimoto KP, Laust AK, Wang K, et al. Restricted and selective tropism of a Venezuelan equine encephalitis virus-derived replicon vector for human dendritic cells. Viral Immunol. 2007; 20(1): 88–104. [PubMed: 17425424]
36. Goldberg SM, Bartido SM, Gardner JP, et al. Comparison of two cancer vaccines targeting tyrosinase: plasmid DNA and recombinant alphavirus replicon particles. Clin Cancer Res. 2005 Nov 15; 11(22):8114–21. [PubMed: 16299244]
37. Morse MA, Hobeika AC, Osada T, et al. An alphavirus vector overcomes the presence of neutralizing antibodies and elevated numbers of Tregs to induce immune responses in humans with advanced cancer. J Clin Invest. 2010 Sep; 120(9):3234–41. [PubMed: 20679728]
38. Durso RJ, Andjelic S, Gardner JP, et al. A novel alphavirus vaccine encoding prostate-specific membrane antigen elicits potent cellular and humoral immune responses. Clin Cancer Res. 2007 Jul 1; 13(13):3999–4008. [PubMed: 17606734]
39. Garcia-Hernandez ML, Gray A, Hubby B, Kast WM. In vivo effects of vaccination with six-transmembrane epithelial antigen of the prostate: a candidate antigen for treating prostate cancer. Cancer Res. 2007 Feb 1; 67(3):1344–51. [PubMed: 17283172]
40. Garcia-Hernandez ML, Gray A, Hubby B, Klinger OJ, Kast WM. Prostate stem cell antigen vaccination induces a long-term protective immune response against prostate cancer in the absence of autoimmunity. Cancer Res. 2008 Feb 1; 68(3):861–9. [PubMed: 18245488]
41. Avogadri F, Zappasodi R, Yang A, et al. Combination of alphavirus replicon particle-based vaccination with immunomodulatory antibodies: therapeutic activity in the B16 melanoma mouse model and immune correlates. Cancer Immunol Res. 2014 May; 2(5):448–58. [PubMed: 24795357]
42. Elzey BD, Siemens DR, Ratliff TL, Lubaroff DM. Immunization with type 5 adenovirus recombinant for a tumor antigen in combination with recombinant canarypox virus (ALVAC) cytokine gene delivery induces destruction of established prostate tumors. Int J Cancer. 2001 Dec 15; 94(6):842–9. [PubMed: 11745487]
43. Eriksson M, Andreasson K, Weidmann J, et al. Murine polyomavirus virus-like particles carrying full-length human PSA protect BALB/c mice from outgrowth of a PSA expressing tumor. PLoS One. 2011; 6(8):e23828. [PubMed: 21858228]
44. Hannan R, Zhang H, Wallecha A, et al. Combined immunotherapy with Listeria monocytogenes-based PSA vaccine and radiation therapy leads to a therapeutic response in a murine model of prostate cancer. Cancer Immunol Immunother. 2012 Dec; 61(12):2227–38. [PubMed: 22644735]
45. Klyushnenkova EN, Riabov VB, Kouiavskaia DV, et al. Breaking immune tolerance by targeting CD25+ regulatory T cells is essential for the anti-tumor effect of the CTLA-4 blockade in an HLA-DR transgenic mouse model of prostate cancer. Prostate. 2014 Oct.74:1423–32. [PubMed: 25111463]
46. Riabov VB, Kim D, Chhina S, Alexander RB, Klyushnenkova EN. Immunostimulatory early phenotype of tumor-associated macrophages does not predict tumor growth outcome in an HLA-DR mouse model of prostate cancer. Cancer Immunol Immunother. 2015 Apr. (in press).

Highlights

- Alphavirus-based virus-like particle vector (VLPV) encoding human Prostate-Specific Antigen (PSA) was tested in a stringent “humanized” double-transgenic mouse model of prostate cancer
- VLPV-PSA induced a robust PSA-specific cellular and humoral immune response *in vivo*.
- Tumor growth in VLPV-PSA vaccinated mice was significantly delayed at early time points.
- VLPV-PSA vaccine can efficiently overcome immune tolerance to PSA and mediate rapid clearance of PSA-expressing tumor cells

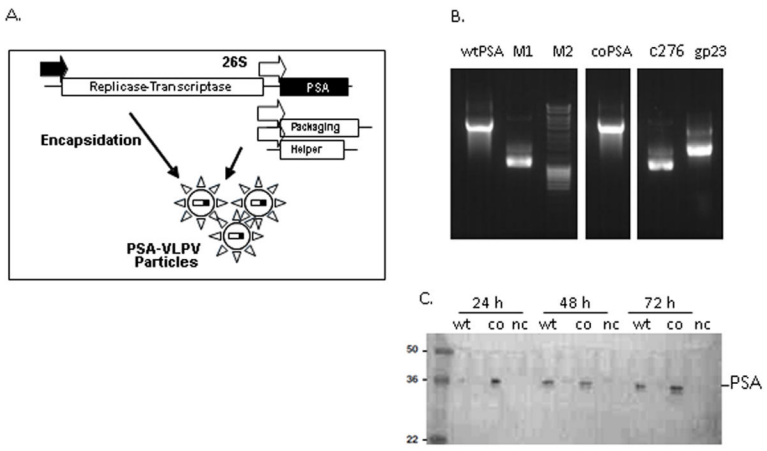

Figure 1. VLPV-PSA vaccine design

A. *Schema of the TC-83 vaccine replicon vector containing cloned PSA gene, and a bipartite packaging helper*. Indicated are the T7 RNA polymerase promoter (filled arrow), the 26S subgenomic promoter (open arrows), and the location of the PSA gene in the vaccine vector. **B.** *Production of RNA for transfection into CHO cells.* RNAs were made by run-off *in vitro* transcriptions using T7 RNA polymerase in the presence of 5′ cap analog. The order of the samples as follows: wild-type PSA (wtPSA); M1 and M2, RNA and DNA control markers; codon-optimized PSA (coPSA); C276 c-helper and gp23 gp-helper. **C**. *Expression of PSA by Western blot.* CHO-K1 cells were transfected with vector RNA encoding PSA variants, culture supernatants were collected at indicated time points. Western blot was carried out using antiserum specific for human PSA. “wt”, “co”, “nc” indicate wtPSA, coPSA, and negative control respectively.

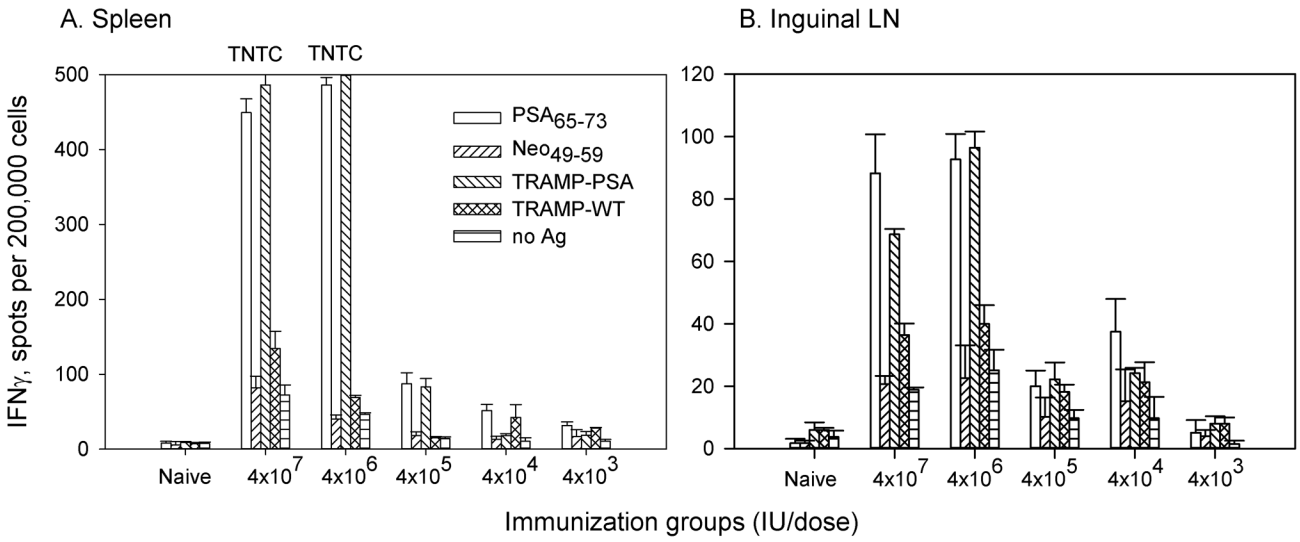

Figure 2. VLPV-PSA vaccine induces dose-dependent PSA-specific immune response in DR2bxPSA F_1 mice

Mice were immunized i.m. twice with VLPV-PSA at indicated doses. Cellular immune responses to PSA were measured in the spleens (A) and inguinal LN (B) two weeks after boost immunization using IFNγ ELISPOT assay. Lymphocytes (2×10^5 per well) were stimulated with either H-2D^b restricted peptide $PSA_{65–73}$ or TRAMP-PSA tumor targets. Irrelevant peptide $Neo_{49–59}$, parental TRAMP-C1 tumor cells or media (No Ag) were used as negative controls. Target tumor cells were pre-treated with IFNγ and irradiated at 10,000 rad. The data for the pool of 3 mice per group are shown (mean ± SD of triplicates). TNTC: too numerous to count.

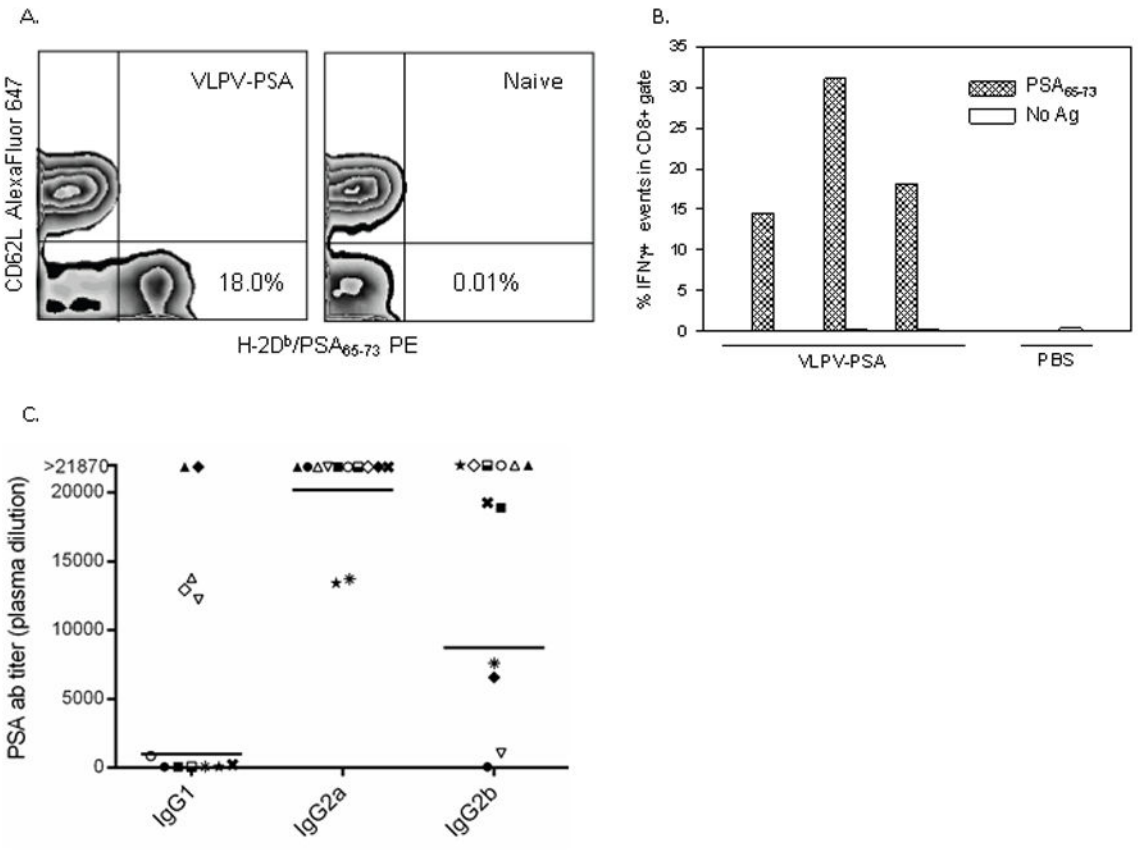

Figure 3. Immunogenicity of VLPV-PSA vaccine in DR2bxPSA F_1 mice

A. *Direct detection of PSA-specific CD8+ T cells in the peripheral circulation*. Peripheral blood was stained with H-2D^b/PSA$_{65–73}$ Dxt PE in combination with anti-CD8 FITC and CD62L Alexa Fluor 647 mAbs. Percentages of the Dxt+CD62L− events within CD8+ gate are shown for a representative VLPV-PSA-vaccinated (*left panel*) or naïve (*right panel*) mouse. **B.** *Intracellular cytokine staining.* Splenocytes were stimulated for 16 hr with H-2D^b-restricted peptide PSA$_{65–73}$ or left untreated (No Ag). Cells stimulated with PMA/Ionomycin were used as positive controls (data not shown). Cells were stained with anti-CD8 PerCP Cy5.5 mAb followed by intracellular staining with anti-IFNγ PE mAb. Percentages of events within CD8+ gate are shown for individual mice from a representative experiment. **C**. *Anti-PSA antibody responses.* Heparinized plasma was analyzed for the presence of anti-PSA Abs by ELISA. Anti-PSA ab titers are shown for IgG1, IgG2a, and IgG2b sub-isotypes. Each symbol represents a titer for an individual mouse (n=12). Horizontal lines are geometric means. For the titers above assay upper limit of quantitation values equal to 21,870 were designated.

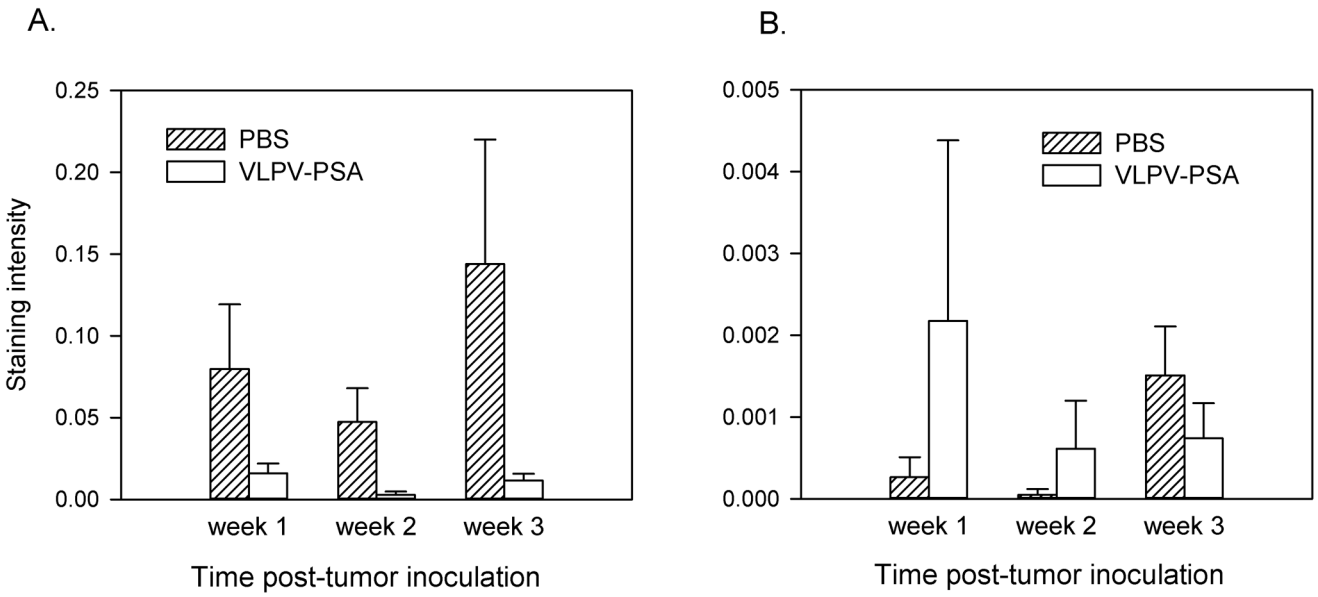

Figure 4. The kinetics of PSA expression and CD8 T cell infiltration in TRAMP-PSA tumors

Mice were immunized with VLPV-PSA followed by the inoculation with TRAMP-PSA tumor cells impregnated in Matrigel. Tumor implants were harvested 1, 2 or 3 weeks later (n=3 per treatment group per time point). Cryosections were stained using either goat anti-human PSA (**A**) or rat anti-mouse CD8 (**B**) Abs. Images were taken using Zeiss Axioskop microscope with 2.5X objective using AxioVision 3.0 software. Images were scanned using Aperio ImageScope software and Positive Pixel Count Algorithm. Data are expressed as average intensity of staining (positivity) ± SD. Representative IHC images for individual mice are shown in Supplemental Figure 2 (PSA) and Supplemental Figure 3 (CD8). The global effect of the vaccination analyzed by the ANOVA F test was statistically significant for the PSA staining intensity (**A**) ($p=0.0007$), although pairwise comparisons between vaccinated and non-vaccinated groups at each time point were only marginally significant ($0.05<p<0.1$, Satterthwaite t-test). The global effect of the vaccination for the CD8 staining intensity (**B**) was not significant ($p=0.347$). Within the treatment groups, the effect of time was also non-significant (ANOVA F test).

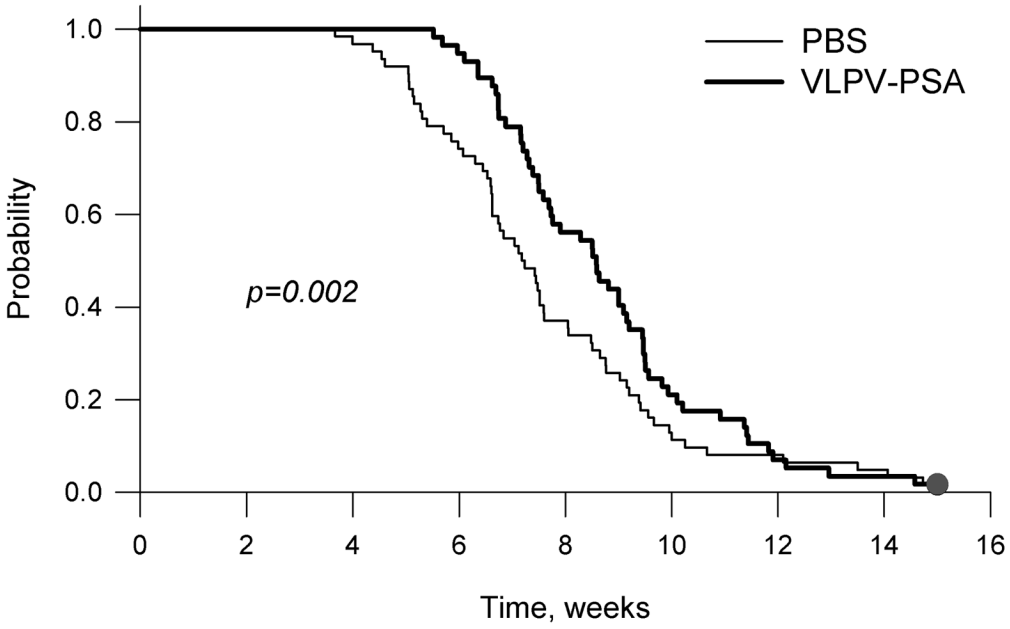

Figure 5. Vaccination with VLPV-PSA delays tumor growth at early time-points

Mice were immunized with VLPV-PSA vaccine twice with 4 weeks interval between primary and secondary immunizations. Four weeks after secondary immunization mice were s.c. injected with TRAMP-PSA tumor cells. Tumor growth was monitored weekly for up to 15 weeks. Combined results from 4 independent experiments with identical trend are shown (n=62 for the control group, n=57 for the vaccine group). *Time-to-event analysis* (tumor base of 100 mm^2) was performed by the Gehan-Breslow test (p value is shown on the graph). The results of the individual experiments are shown in Table 1.

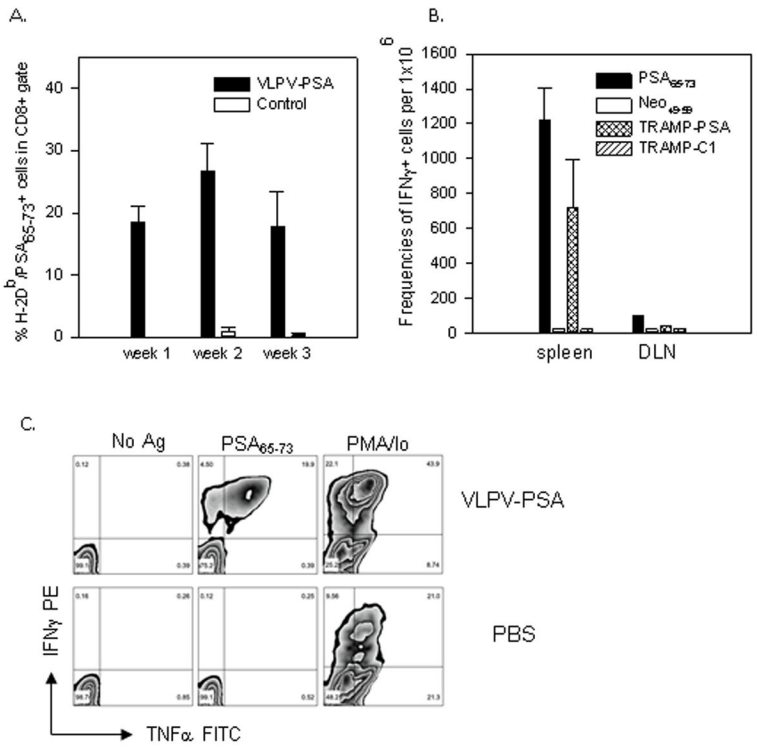

Figure 6. PSA-specific CD8 T cell response after TRAMP-PSA tumor inoculation

Mice were immunized with VLPV-PSA followed by the s.c. injection with TRAMP-PSA tumor cells. **A.** *The kinetics of PSA-specific CD8 T cell response in the peripheral blood.* Heparinized blood was collected at indicated time points after tumor inoculation and stained with H-2D^b/PSA$_{65–73}$ Dxt PE, anti-CD8 FITC, and CD62L Alexa Fluor 647 mAbs. Percentages of the Dxt+CD62L− events within CD8+ gate are shown. The difference between week 1 and week 2 was statistically significant (ANOVA F test, p=0.04). The data are averages ± SD (n=3 per group). **B.** *IFNγ ELISPOT assay.* Splenocytes from individual mice (2×10^5 per well, n=3) or DLN pooled from the same mice (4×10^5 per well) were plated in triplicates and stimulated with either H-2D^b restricted peptide PSA$_{65–73}$ or TRAMP-PSA tumor targets. Irrelevant peptide Neo$_{49–59}$, parental TRAMP-C1 tumor cells or media (No Ag) were used as negative controls. Frequencies of the IFNγ-producing cells per 1×10^6 were calculated as described in the "Materials and Methods" section. **C.** *Intracellular cytokine staining.* Splenocytes were stimulated as described in the legend to Figure 2B. Cells were stained with anti-CD8 PerCP Cy5.5 mAb followed by intracellular staining with anti-IFNγ PE and anti-TNFα FITC mAbs. The dot plots for the representative vaccinated and control mouse are shown. Numbers are percentages of events in each quadrant within CD8+ gated population.

Table 1

Time to-event analysis (tumor base area 100 mm^2) for the TRAMP-PSA tumor growth in mice vaccinated with VLPV-PSA.

		Experiment 1	Experiment 2	Experiment 3	Experiment 4	Combined
PBS	Median (95% CI)	7.5 (7.1, 7.9)	6.6 (5.0, 8.2)	9.2 (7.8, 10.7)	6.1 (5.5, 6.6)	7.2 (6.5, 7.9)
	N	21	15	14	12	62
VLPV-PSA	Median (95% CI)	8.6 (8.2, 9.0)	7.5 (7.2, 7.8)	11.3 (9.5, 13.2)	7.2 (6.4 – 7.9)	8.6 (7.6, 9.5)
	N	15	15	15	12	57
Gehan-Breslow p value		*0.097*	*0.116*	*0.05*	*0.023*	*0.002*
Log rank p value		*0.419*	*0.427*	*0.294*	*0.023*	*0.059*

Mice were vaccinated as described in the legend to Figure 5. The Kaplan-Meier survivor curves for the combined data are shown in Figure 5.